Oncogene (2000) 19, 2803–2811

www.nature.com/onc

Tracheal development and the von Hippel–Lindau tumor suppressor homolog in *Drosophila*

Boris Adryan[1,3], Hans-Jochen H Decker[3], Takis S Papas[1,4] and Tien Hsu*[,1,2]

[1]*Center for Molecular and Structural Biology and Hollings Cancer Center, Medical University of South Carolina, Charleston, South Carolina, SC 29425, USA;* [2]*Department of Cell Biology and Anatomy, Medical University of South Carolina, Charleston, South Carolina, SC 29425, USA;* [3]*Department of Hematology and Oncology, Johannes-Gutenberg University of Mainz, Obere Zahlbacher Str. 63, D-55131 Mainz, Germany*

von Hippel–Lindau disease is a hereditary cancer syndrome. Mutations in the *VHL* tumor suppressor gene predispose individuals to highly vascularized tumors. However, *VHL*-deficient mice die *in utero* due to a lack of vascularization in the placenta. To resolve the contradiction, we cloned the *Drosophila VHL* homologue (*d-VHL*) and studied its function. It showed an overall 50% similarity to the human counterpart and 76% similarity in the crucial functional domain: the elongin C binding site. The putative d-VHL protein can bind *Drosophila* elongin C *in vitro*. During embryogenesis, *d-VHL* is expressed in the developing tracheal regions where tube outgrowth no longer occurs. Reduced *d-VHL* activity (using RNA interference methodology) caused breakage of the main vasculature accompanied by excessive looping of smaller branches, whereas over-expression caused a general lack of vasculature. Importantly, human *VHL* can induce the same gain-of-function phenotypes. VHL is likely involved in halting cell migration at the end of vascular tube outgrowth. Loss of VHL activity can therefore lead to disruption of major vasculature (as in the mouse embryo), which requires precise cell movement and tube fusion, or ectopic outgrowth from existing secondary vascular branches (as in the adult tumors). *Oncogene* (2000) **19**, 2803–2811.

Keywords: *Drosophila*; tracheal development; *VHL*; vascularization

Introduction

Germline mutations in the von Hippel–Lindau tumor suppressor gene (*VHL*) and somatic inactivation of the other allele result in highly vascularized tumors such as clear cell renal carcinoma, retinal angioma and hemangioblastomas of the central nervous system (for reviews, see Gnarra *et al.*, 1996; Kaelin and Mahler, 1998).

The human *VHL* (*h-VHL*) gene encodes two polypeptides of 213 and 160 amino acids, resulting from in-frame alternative start codon usage (Latif *et al.*, 1993; Iliopoulos *et al.*, 1998). Although there is no extensive homology between VHL and other known proteins, recent studies have shown that VHL, together with elongin B/C, cullin-2 and Rbx1, forms an E3 ubiquitin ligase complex (Iwai *et al.*, 1999; Kamura *et al.*, 1999; Lisztwan *et al.*, 1999; Pause *et al.*, 1999). Thus, VHL may be involved in recognizing specific protein targets and mediate their degradation through ubiquitination.

The best characterized VHL function thus far has been its involvement in hypoxia-induced angiogenesis. Supporting this functional role is the identification of one of its degradation targets: the α subunit of the hypoxia-inducible factor 1 (Hif-1 α; Wang *et al.*, 1995; Maxwell *et al.*, 1999). Hif-1 is a transcription activator that mediates the hypoxia-induced up-regulation of vascular endothelial growth factor (VEGF) expression (Maxwell *et al.*, 1997), which is a potent inducer of angiogenesis (Leung *et al.*, 1989; Shweiki *et al.*, 1992). VHL can therefore be considered an anti-angiogenic factor and this function can explain the over-vascularized phenotypes in the VHL tumors.

However, this view was inconsistent with the finding that germline *VHL* knockout mice showed embryonic lethality due to a lack of vascularization in the placenta (Gnarra *et al.*, 1997). In an attempt to resolve this apparent contradiction, we sought to study the *VHL* function in an experimentally accessible *in vivo* system, *Drosophila melanogaster*. We showed that the *Drosophila VHL* (*d-VHL*) is highly conserved as compared to the human counterpart and has a role in the development of the *Drosophila* vasculature, the tracheal system. Reduction of *d-VHL* activity can either disrupt or induce vascular growth, depending on the nature of the tracheal branches. A model for the *d-VHL* function is proposed that underlies the seemingly contradictory phenotypic outcomes.

Results

Cloning of the d-VHL *gene sequence*

A segment of the human *h-VHL* open reading frame (ORF) corresponding to amino acid residues 59–208 was used as a query to search the Berkeley *Drosophila* Genome Project database (http://www.fruitfly.org). An uninterrupted *VHL*-like ORF was identified within two P1 contigs DS00724 and DS00284 (GenBank accession #AC006066) encompassing the chromosomal 2R region 47D6–47E6. In order to determine whether or not the identified sequence is transcribed *in vivo*, reverse transcription-coupled polymerase chain reaction (RT–PCR) was performed on either ovarian or embryonic RNA samples. Both produced cDNA fragments of expected size of about 600 base-pairs.

*Correspondence: T Hsu, Center for Molecular & Structural Biology, HCC 334, Medical University of South Carolina, 86 Jonathan Lucas St., Charleston, SC 29425, USA
[4]This work is dedicated to the memory of Dr Takis S Papas
Received 11 January 2000; revised 6 April 2000; accepted 6 April 2000

They were confirmed by sequence analysis to be identical to the genomic sequence. Therefore there are no small introns embedded in the ORF.

The candidate 178-amino acid d-VHL protein can be aligned along its entire length with the smaller of the two h-VHLs (Figure 1a; Gnarra *et al.*, 1994; Beroud *et al.*, 1998; Stebbins *et al.*, 1999). d-VHL has an overall 22% identity to h-VHL and is 50% similar when conserved amino acid changes were considered (Figure 1b). In the two functionally significant protein interaction domains, human residues 113–121 and 157–172 that encompass the protein kinase C λ (PKCλ) and the elongin C binding sites, respectively (Okuda *et al.*, 1999; Kibel *et al.*, 1995), the conservation is significantly higher at 67 and 76%.

The hallmark of h-VHL activity is its ability to bind elongin C. Since the *Drosophila* elongin C (d-elongin C) has been cloned and it showed over 90% identity to the human counterpart (Aso and Conrad, 1997), we tested whether or not the putative d-VHL can bind to d-elongin C. As shown in Figure 2a, the purified d-VHL can interact with d-elongin C without the presence of other factors such as elongin B. The binding activity of d-VHL appears to be selective since the majority of the protein present in the binding reaction were not bound by d-VHL (Figure 2a, lower panel). It is worth noting that in a similar experiment, d-VHL did not interact specifically with d-elongin B (data not shown). We henceforth consider the isolated VHL-like sequence a true homolog of the mammalian counterparts.

A

```
                                                                  PKCλ binding site
h-VHL MPRRAENWDEAEVGAEEAGVEEYGPEEDGGEESGAEESGPEESGPEELGA  50
                                                                                |
d-VHL ------------------------------------------------MALQI   5

h-VHL EEEEEAGRPRPVL-RSVNSREPSQVIPCNRSPRVVLPVWLNFDGEPQPYP  99
      :. . |:   | : ..:    |:|.| : |.:   |:    . . |
d-VHL AQNNRDGQ---QLVGADQGKVEVYVLFANTTYRTLDLYWVCERERENMYL  52

                    PKCλ binding site
h-VHL TLPPGTGRRIHSYRGHLWLFRDAGTHDGLLVNQTELFVPSL----NVDGQ 145
      || |   |::::  | |||||  | : : |.. .:| |      . . .
d-VHL TLKPFEEVRVNTPTTHSWLFRDYYTGKRMHVRSQRIPQPIRVRVPKSQQS 102

                                Elongin C binding site
h-VHL P----IFAN---ITLPVYTLKERCLQVV-RSLVKPENY-RRLDIVRSLYE 186
      |      :   | .|: :|:|.|| :| | |:: :|  ||:    : .
d-VHL PDQLVDVRSEVLIHFPMRSLRENCLWLVARWLIRTSNAPRRIIHGYHIPS 152

h-VHL DLEDHPNVQKDLERLTQERIAHQRMGD 213
      |:..      . : .|:|  |
d-VHL TLKQQLLSLLTCIE-SYSRVAGTRRRR 178
```

B

hVHL/dVHL	Identity	Similarity
Overall	22%	50%
PKCλ binding site	67%	67%
Elongin C binding site	41%	76%

Figure 1 Conservation of the VHL proteins. (**a**) Amino acid sequence alignment (Henikoff and Henikoff, 1992) of the VHL proteins from human (h-VHL) and *Drosophila* (d-VHL). Identical residues are marked by vertical lines and similar residues are marked by (:) or (.), according to the degree of similarity. The alternative initiation codon for h-VHL is highlighted. Boxed residues are those identified as minimally required for specific protein interaction as indicated. (**b**) Extent of homology between *Drosophila* and human VHL proteins

d-VHL was then mapped more precisely to a single polytene chromosomal position at 47E1-3 (Figure 2b), consistent with the location of the P1 clones. Two transcripts of 1.4 and 1.2 kb were detected in developmental Northern analysis (Figure 2c). The gene is expressed at low levels in embryo, pupa, and adults, and at a very low level in larva. One cDNA clone of 1.287 kb was subsequently isolated from an ovarian library (Stroumbakis *et al.*, 1994). Sequence analysis (submitted to GenBank, accession #AF195836) showed that there are no introns in the 141 bp 5′ or the 669 bp 3′ untranslated regions.

Expression pattern of d-VHL

Whole-mount RNA *in situ* hybridization was performed on the developing embryos in order to assess the function of *d-VHL*. In the first 12 h of development at 25°C (stages 1–14), there is no specific tissue staining, although an above-background general staining is observed (Figure 3a,b). At stage 15, or ~12–13 h after egg laying, specific staining appears in the main dorsal trunk of the tracheal system (Figure 3c) and gradually progresses into other, smaller branches at later stages (Figure 3d,e). This temporal pattern appears to lag behind the progression of branching outgrowth in the trachea. This is best illustrated when the *d-VHL* expression pattern is compared to that of the Trachealess (Trh) protein, a transcription factor with structural similarity to the mammalian Hif-1 α (Wilk *et al.*, 1996). Trh is expressed in all tracheal cells throughout tracheal development, starting from the formation of 10 trachea-forming subunits, termed tracheal placodes, on each side of the germband at stage 11. Cells within each tracheal placode invaginate from the epithelium and start branching and outgrowth at stage 12 (Figure 3f). The largest tracheal tubes, the dorsal trunks (DT), are formed by horizontal fusion of the elongating tracheal subunits (Figure 3f,g). The fusion of DT is nearly complete at stage 14 (Figure 3g) while other cells continue to migrate perpendicularly to DT to form smaller branches. About 1–2 h later, at stage 15, the DT formation is complete (Figure 3h) and other branches continue to extend through stage 16 and 17 until the embryos mature (Figure 3i,j). During this process, *d-VHL* expression appears only in the tracheal regions where cell migration and tube outgrowth no longer occur. This suggests that *d-VHL* may be involved in halting cell movement within the tracheal system. In light of this model, it is interesting to point out that *d-VHL* is expressed at a very low level at the larval stage (Figure 2b), when extensive tracheal tube outgrowth is needed to keep pace with the rapid growth of body masses.

A role of *d-VHL* in regulating tracheal cell proliferation is not favored since the number of tracheal cells remains constant throughout tracheal development (Samakovlis *et al.*, 1996) while *d-VHL* expression only appears at stage 15. Tube formation results solely from cell migration and elongation.

d-VHL *loss-of-function phenotypes*

Since there are no genomic mutations of *d-VHL*, we sought to study the *in vivo* function by using RNA interference (RNAi) methodology, a gene silencing

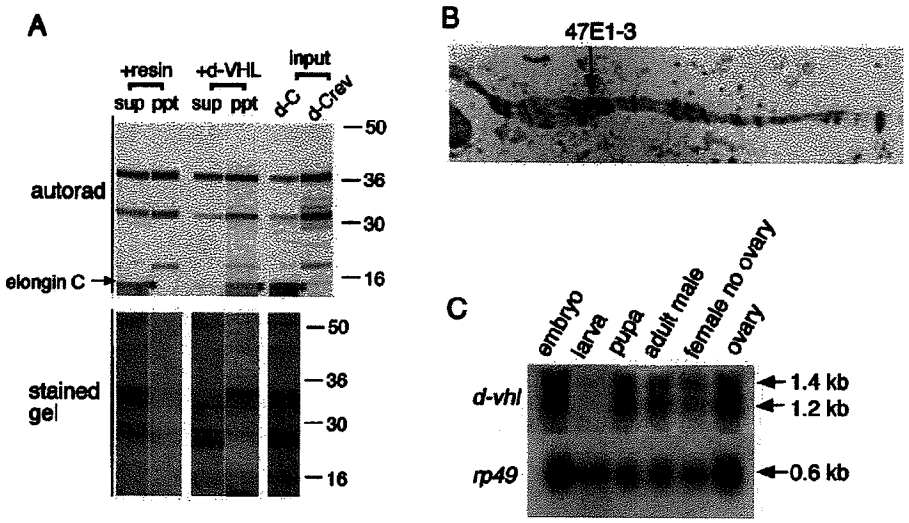

Figure 2 Structure and activity of *d-VHL*. (**a**) Binding to *Drosophila* elongin C. Top panel: autoradiogram of labeled proteins. In coupled transcription/translation reactions, proteins were made from either sense (d-C) or antisense (d-Crev) direction of the d-elongin C plasmid clone, in the presence of ^{35}S-methionine (see Materials and methods). The putative d-elongin C of predicted size (~12 kD) is present in the d-C sample (marked by an asterisk). Other labeled proteins were either from the RNAs present in the reticulocyte lysate or from the antisense *d-elongin C* sequence. The two samples were both added to either resin-bound d-VHL or the resin alone. The protein species other than d-C served as internal controls for monitoring specific binding. The unbound (sup) and the bound (ppt) protein species were separated on a 10–15–20% step-gradient gel and detected by autoradiography. The molecular weight markers on the right are in kD. Lower panel: Coomassie blue-stained gel corresponding to the lanes in the top panel. Resin alone did not precipitate detectable amounts of major protein species in the reticulocyte lysate. Importantly, d-VHL did not indiscriminately precipitate all the proteins. (**b**) Polytene chromosomes hyrbidized with a digoxygenin-labeled *d-VHL* probe. The hybridization signal is located at position 47E1-3 (arrow) of the chromosome arm 2R. (**c**) Northern analysis of total RNA samples from various developmental stages. The ^{32}P-labeled *d-VHL* probe and a probe corresponding to the ribosomal protein 49 gene (*rp49*) were used. The latter served as a loading control. Sample sources are indicated on top. Note that the autoradiographic exposure time for the *d-VHL* probe is 10 days as compared to 8 h for the comparably-labeled *rp49* probe

strategy mediated by double-stranded (ds) RNA (Fire *et al*., 1998; Kennerdell and Carthew, 1998). ds RNA encompassing the coding region of *d-VHL* was produced *in vitro* and injected into embryos. ds *lacZ* RNA was used as a negative control. The effects of RNAi on reducing the level of the endogenous *d-VHL* RNA was monitored by RNA *in situ* hybridization (compare Figure 4c′ with Figure 4a′).

Distinctive tracheal phenotypes were observed (Figure 4 and Table 1). The most striking phenotype is the ectopic and excessive branching and looping of the smaller tracheal branches, accompanied by breakage of dorsal trunks (Figure 4c–e; compare with Figure 4a,b). In one example (Figure 4c), an ectopic transverse connective (TC) grew out of an over-extended visceral branch (VB), while branches of the lateral trunks (LT) showed abnormal looping. Interestingly, the ectopic branching and looping observed here resemble the hypoxia response demonstrated in *Drosophila* (Jarecki *et al*., 1999; Wingrove and O'Farrell, 1999).

The largest tubes in the tracheal system, the dorsal trunks (DT), appeared to respond differently from the other tubes to *d-VHL* loss-of-function. As suggested by the RNA expression pattern, *d-VHL* may be involved in halting tracheal cell movement after tube outgrowth is complete. This may be particularly important for the dorsal trunk, which requires precise lateral outgrowth and interconnection from 10 axially laid out subunits (Figure 3f–h). When *d-VHL* activity is inhibited, DT cells may continue moving and/or migrate ectopically without fusing with the opposing tubes. On the contrary, the smaller branches grow out from existing tubes and have free migrating ends. Uncontrolled cell migration in these branches can therefore result in excessive and ectopic looping and branching.

In support of this model, we also observed ectopic migration of Trh-expressing cells in *d-VHL* dsRNA-injected embryos, at the expense of DT formation (Figure 3k).

d-VHL *gain-of-function phenotypes*

If the proposed function of *d-VHL* is correct, one prediction would be that, in a gain-of-function *d-VHL* mutant, DT formation will also fail since cell migration is inhibited. The difference from the loss-of-function mutant would be a reduced capability of the small branches to produce additional outgrowth. In other words, there will be a general lack of vascularization.

The gain-of-function mutant was generated by injecting the embryos with capped sense *d-VHL* RNA. It was immediately obvious that the RNAi phenotype described above occurred only at the background level (Table 1). The other seemingly varied phenotypes appeared to be different extents of the same theme, i.e., repressed tracheal development. Two examples are shown: no tracheae at all (Figure 4f) and broken dorsal trunk without smaller branches (Figure 4g). The over-expression was monitored by RNA *in situ* hybridization, which showed excessive sense RNA accumulation at stage prior to normal tracheal expression of the endogenous *d-VHL* (compare Figures 4f′ with 3b′). Capped sense *lacZ* RNA was used as a negative control and it showed no specific effects (Table 1).

In order to determine whether or not *h-VHL* is functionally equivalent to *d-VHL*, the *h-VHL* sense

RNA was injected into the embryos. Significantly, *h-VHL* could induce the similar gain-of-function phenotype (Figure 4h and Table 1). Over-expression of *h-VHL* was monitored by RNA *in situ* hybridization (Figure 4h′). It is worth noting that *h-VHL* has recently been shown to inhibit branching morphogenesis of the renal carcinoma cells (Koochekpour *et al*., 1999). Lack of cell movement in these mutants could also be

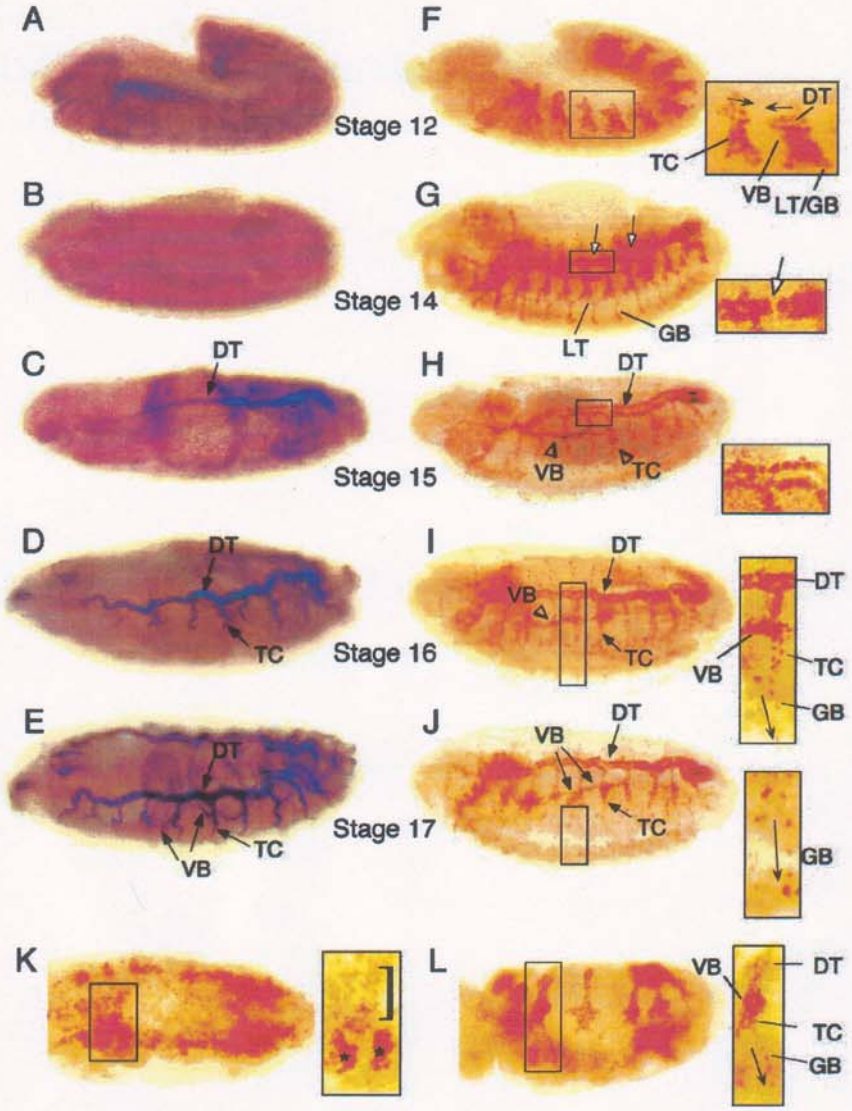

Figure 3 *d-VHL* RNA expression in the tracheal system. Unless specified, all embryos are shown in lateral view and anterior is to the left. (**a–e**) Wild-type embryos (strain Oregon-R) were hybridized with digoxigenin-labeled *d-VHL* antisense RNA probe. Sense *d-VHL* RNA probe was used in the RNA *in situ* experiment as a negative control and it showed no specific staining (unpublished observations). (**f–j**) Comparably staged embryos are stained with anti-Trh antibody to show all tracheal cell nuclei. (**a–j**) Embryos of the same stage are aligned horizontally as indicated in the middle. (**a–b**) *d-VHL* is not expressed in the trachea up to stage 14. (**c**) The expression first appears at stage 15 in the dorsal trunk (DT). (**d,e**) The expression then progresses into finer branches such as transverse connective (TC) and visceral branch (VB). (**e**) is in dorsal-lateral view. (**f**) Two tracheal placodes are highlighted. The arrows in the enlarged section point to the directions of cell migration that leads to DT formation. Future tracheal branches are marked in the corresponding regions of the tracheal placodes (enlarged view). LT/GB denotes the origin of the future lateral trunk and gaglionic branch. (**g**) The open arrows point to the yet to be connected junctions in DT. Lateral trunk (LT) and gangalionic branch (GB) are indicated. (**h**) DT connection is complete at stage 15. (**h,i**) Open arrowheads point to the extending branches that do not express *d-VHL* (compare to **c** and **d**). (**h–j**) The dark arrows point to the completed tracheal branches that also express *d-VHL* (compare to **c–e**). Enlarged section in (**i**) highlights the mature tracheal branches (compare to **f**). The arrow marks the movement of the extending GB. Enlarged section in (**j**) shows migrating GB cell nuclei. (**k**) Anti-Trh antibody staining of a stage 16 embryo injected with *d-VHL* double-stranded RNA (dorsal view). Bracket in the enlarged section indicates the ectopically migrating cells. Asterisks indicate the remnants of the tracheal placodes. No DT is formed in this region. (**l**) Anti-Trh antibody staining of a stage 16 embryo injected with *d-VHL* sense RNA. Most of the tracheal cells are still within the tracheal placodes. Enlarged section shows that only a few cells have migrated to form GB (arrow) while most other cells remain in the tracheal placode without forming any branches (compare to **f** and **i**)

observed when tracheal cells were marked by anti-Trh antibody (Figure 3l). At stage 16, while some cells migrated out, most tracheal cells remained in the original tracheal placodes.

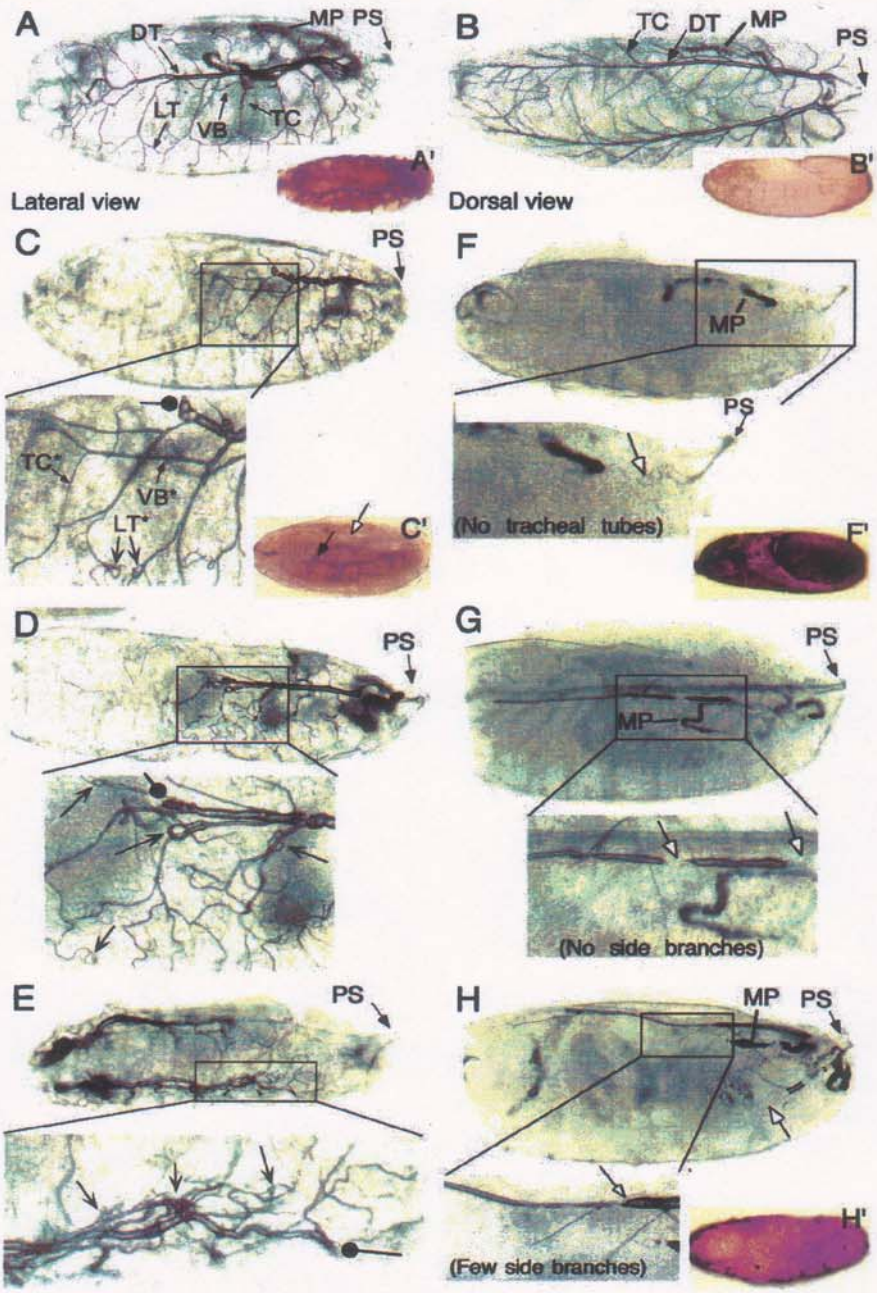

Figure 4 Tracheal phenotypes of the *VHL* loss-of-function and gain-of-function mutants. Embryos were injected with double-stranded (ds) *lacZ* RNA (**a**), capped sense *lacZ* RNA (**b**), *d-VHL* ds RNA (**c–e**), capped sense *d-VHL* RNA (**f,g**), or capped sense *h-VHL* RNA (**h**). The embryos were directly observed under a light microscope. Posteriors of the embryos are oriented to the right. (**a,c,d,f,g,h**) are shown in lateral views whereas (**b**) and (**e**) are in dorsal views. Relevant tracheal structures are indicated in (**a**) and (**b**). DT: dorsal trunk; LT: lateral trunk; PS: posterior spiracle; TC: transverse connective; VB, visceral branch. Also visible is the non-trachea tube-like organ Malpiphian tube (MP). In (**c–e**), sharp arrows (→) point to sites of ectopic looping and branching and round pointers (—●) point to ends of the broken dorsal trunk. Asterisks (*) in (**c**) indicate the ectopic branches. Gain-of-function phenotypes in (**f–h**) show no or few tracheal tubes. Open arrows point to broken or terminated dorsal trunks. Inserts in **a,b,c,f,h** (**a′,b′,c′,f′,h′**) show RNA *in situ* hybridization using digoxigenin-labeled antisense *d-VHL* (**a′,b′,c′,f′**) or *h-VHL* (**h′**) RNAs. (**a′**) is a wild-type stage 17 embryo; (**b′**) is a wild-type stage 12 embryo; (**c′**) is a stage 17 embryo showing no *d-VHL* expression in one set of the tracheal tubes (open arrow) or reduced expression in the other (solid arrow); and (**f′**) and (**h′**) show stage 11–12 embryos with elevated *VHL* expression in almost all cells

Table 1 Quantitation of the *VHL* mis-expression phenotypes[a]

RNA species	*ds* lacZ	*ds* d-VHL	lacZ *sense*	d-VHL *sense*	h-VHL *sense*
Total injected	314	641	400	591	627
Undeveloped[b]	201	352	229	360	431
Sub-total	113	289	171	231	196
Premature death[c]	32 (28.3%)	169 (58.5%)	45 (26.3%)	60 (26.0%)	76 (38.8%)
Tracheal phenotype[d]:					
Broken trunk, ectopic branching	2 (1.8%)	92 (31.8%)	–	6 (2.6%)	12 (6.1%)
No tracheae	–	–	–	17 (7.4%)	12 (6.1%)
Broken trunk, few or no branches	–	–	–	33 (14.3%)	13 (6.6%)
Thin trunk, missing branches, etc	–	–	4 (2.3%)	24 (10.4%)	19 (9.7%)
Total tracheal phenocopies	2 (1.8%)	92 (31.8%)	4 (2.3%)	80 (34.6%)	56 (28.6%)

[a]Quantitation was based on the experiments described in Figure 4. [b]Large numbers of embryos did not survive the injection. These are designated 'undeveloped' and could be identified by their failure to develop any cuticular and internal structures. [c]'Premature death' denotes those that failed to develop to term. Included in this category are those exhibiting obvious early patterning defects in axis determination and mesodermal differentiation. About 28% of *lacZ*-injected embryos are of this category. This represents a background level of developmental defects induced by injecting foreign substances. A higher level of premature death is observed in *d-VHL* ds RNA samples, indicating an additional role of *d-VHL* in early embryonic development. These are not counted as direct tracheal detects. [d]Only those developed past stage 15, judged by morphological landmarks such as discernible midgut and posterior spiracles (see Figure 4) were scored for tracheal phenotypes

Discussion

Structural and functional conservation between Drosophila *and human* VHLs

In this study, we showed the identification of the *Drosophila* homolog of the human VHL tumor suppressor gene. This is supported by the high degree of structural similarity (50% overall) between the two presumptive protein sequences. Significantly, the amino acid conservation is spread throughout the entire length of d-VHL (Figure 1a). In the functionally significant domains of PKC λ and elongin C binding domains, the similarity is much higher at 67 and 76%, respectively (Figure 1b). Indeed, the *Drosophila* VHL homolog can interact with the *Drosophila* elongin C, an essential function ascribed to the VHL protein (Figure 2a). One outstanding distinction between the two proteins, however, is that d-VHL lacks the N-terminal extension found in the larger form of the h-VHL. *h-VHL* gene encodes two biologically active proteins as a result of in-frame alternative AUG codon usage (Gnarra *et al.*, 1994; Beroud *et al.*, 1998; Stebbins *et al.*, 1999). However, no functional significance has been assigned to the extra 53 amino acids at the N-terminus of the large h-VHL. Underlying this fact are the following observations: First, the short h-VHL is sufficient for the tumor suppressor function (Schoenfeld *et al.*, 1998; Blankenship *et al.*, 1999). Second, no clinically relevant mutations have been mapped in the N-terminus (Beroud *et al.*, 1998). Third, the human N-terminal extension is not found in either of the two rodent (mouse and rat) VHLs. Finally, while the second initiation codon for h-VHL is flanked by a highly conserved Kozak initiation signal, the first initiation codon lacks such motif (Schoenfeld *et al.*, 1998).

The structural similarity between the human and the fly VHLs has been borne out by functional substitution of d-VHL by the human counterpart in the gain-of-function phenotypic study (Figure 4; also see below).

Genomic structure of d-VHL

d-VHL was mapped to the chromosomal position 47E1-3 (Figure 2b), consistent with the genomic source of the P1 contigs where *d-VHL* was originally identified. This region contains a handful of tRNA genes and one recently isolated lethal mutation that also affects border follicle cell migration in the egg chamber (Liu and Montell, 1999). The identity of this potentially interesting gene is not known yet.

The isolation of a nearly full-length cDNA clone of *d-VHL* allowed for an analysis of the gene structure. The 1287 bp cDNA should correspond very closely to the 1.4 kb transcript detected in the Northern blot (Figure 2c) considering that a poly(A) ' tail is added *in vivo*. Unlike *h-VHL*, *d-VHL* has no introns in the ORF or in the 5′ and 3′ UTRs. The significance of this difference is not clear.

Developmental Northern (Figure 2c) showed that *d-VHL* is expressed in all developmental stage with the exception of lava, which requires extensive tracheal outgrowth. Although we show here that *d-VHL* has a major function in tracheal development, we do suspect that *d-VHL* may have other developmental functions. For example, RNAi experiments showed that *d-VHL* deficiency resulted in a higher level of early embryonic lethality (Table 1). The question of whether or not *d-VHL* is involved in modulating cell migration and tubulogenesis in general remains to be answered. It is interesting to note, however, that a weak expression of *d-VHL* RNA was detected in the embryonic salivary glands (unpublished observations), which contain an extensive duct system and requires also the function of the Trh (Isaac and Andrew, 1996).

d-VHL *function in tracheal development*

Studies of *d-VHL* gene function presented here indicate that *d-VHL* is a component in the tracheal development pathway. This observation is of great significance since *Drosophila* trachea is considered an excellent model for the mammalian vasculature. The branching morphogenesis in *Drosophila* and mammals is regulated by growth factors, such as the *Drosophila* Branchless fibroblast growth factor (FGF: Sutherland *et al.*, 1996) and the mammalian FGF and VEGF (reviewed in Folkman and Shing, 1992; Risau, 1997), by cell adhesion molecules such as cadherins (Tanaka-Matakatsu *et al.*, 1996; Carmeliet *et al.*, 1999) and by transcription factors such as the Hif-1-like factors

(Wilk *et al*., 1996; Crews, 1998; Wang *et al*., 1995) and Ets family of proteins (Samakovlis *et al*., 1996; Pardanaud and Dieterlen-Lie'vre, 1993). Importantly, terminal outgrowth in both systems can be influenced by physiological conditions such as hypoxia (Shweiki *et al*., 1992; Jarecki *et al*., 1999; Wingrove and O'Farrell, 1999). This study further strengthens the notion that mammalian vascular and *Drosophila* tracheal systems share the same evolutionary origin, which employ the homologous molecular pathways, including the *VHL* gene functions. More detailed molecular and genetic epistatic analyses are now underway to elucidate the role of VHL in vasculogenesis.

Based on the expression patterns and the phenotype analyses of *d-VHL* mis-expression, we propose that VHL is likely involved in halting cell movement at the end of vascular tube outgrowth. This is supported by the following observations: First, *d-VHL* RNA expression appears only in the fully connected and/or extended tracheal tubes (Figure 3). Second, reduced *d-VHL* function resulted in ectopic looping of tracheal tubes with free migrating ends while disrupting the formation of major tubes requiring precise cell migration and fusion (Figures 3 and 4). Third, over-expression of d-VHL resulted in inhibition of cell migration and, consequently, stunted tracheal tube formation (Figures 3 and 4). This model can explain the two different *VHL* loss-of-function outcomes observed in knockout mice and human tumors. As observed in *Drosophila*, reduction of *vhl* function by RNA interference possibly lead to uncontrolled cell movement and disrupt the primary vasculature that requires stereotypical cell migration and branching. This is likely the analogous situation observed in the germline knockout mice. On the other hand, once the primary vascular structure is laid out, a lack of VHL activity, and hence excessive cell migration and branching, can simply lead to over-vascularization, as observed in the secondary branches of the *Drosophila* tracheae and in human tumors.

What then are the *in vivo* targets of d-VHL? Mammalian VHLs are thought to directly or indirectly down-regulate VEGF expression. However, the VEGF level increased in $VHL^{-/-}$ mice (Gnarra *et al*., 1997). Therefore, the true *in vivo* action of VHL in the vasculo/angiogenic pathway is still unclear. In *Drosophila*, the vasculogenic and hypoxia-responsive factor appears to be Branchless FGF (Sutherland *et al*., 1996). Could d-VHL modulate tracheal cell migration by repressing the expression of *branchless*? Since *d-VHL* is expressed in the tracheal tubes while *branchless* is expressed in the neighboring cells, the true d-VHL target may very well be the FGF receptor gene *breathless*, not the ligand itself. Elucidating this pathway may ultimately shed lights on the mammalian VHL function.

Materials and methods

RT–PCR

The *d-VHL* upstream primer, 5′-CCATTGCAGATCGGCTTAGC, is located at 32 to 13 nucleotides upstream of the initiation codon. The downstream primer, 5′-ACTAACAACTAGGAGTGTGC, is located at 22 to 3 nucleotides downstream of the stop codon. RT–PCR reactions were carried out as described (Hsu *et al*., 1992). Embryonic or ovarian total RNA samples from the *y*, *w* strain were used. The resulting fragments were blunt-end cloned into the *Sma*I site of the pBluescript-KS vector (Stratagene). The two RNA sources yielded identical sequences.

d-VHL protein purification

The *Drosophila* VHL open reading frame (ORF) was cloned into the pET15b vector (from Novagen) for generating histidine-tagged recombinant protein in bacteria. The His-d-VHL protein is insoluble in the bacteria extract and the pellet was dissolved in Ni-column buffer (5 mM imidazole, 0.5 M NaCl, 20 mM Tris-HCl, pH 7.9) in the presence of 6 M guanidine hydrochloride. The protein extract was loaded onto the Ni-agarose column (from Novagen) and purified according to supplier's instructions except that the recombinant protein was renatured by sequential washing with column buffer containing 3, 1.5, 0.75 and 0 M guanidine hydrochloride while bound to the resin. The bound protein was then used for subsequent binding assays. d-VHL protein production was induced by 1 mM of isopropyl-β-thiogalactopyranoside for 3 h at 37 °C. Protein extracts from a 30 ml culture was loaded onto 2.5 ml bed-volume of resin. Total protein yield was ~25 μg or 100 ng per 10 μl of resin.

Elongin C binding assay

The d-VHL-bound resin was made 50% slurry in the binding buffer (40 mM HEPES, pH 7.9, 0.1 M KCl, 1 mM dithiothreitol, 50 mM $ZnSO_4$, 0.1 mM EDTA and 10% glycerol). The *Drosophila* elongin C (d-elongin) ORF was obtained by RT–PCR using specific primers. The DNA fragment was cloned into the pBluescript vector (from Stratagene) and verified by nucleotide sequencing. The protein was synthesized *in vitro* using coupled transcription/translation reactions (TNT Coupled Reticulocyte Lysate Systems from Promega). ^{35}S-methionine was included in the synthesis reaction to label the protein product. 1 μg of the d-elongin-containing plasmid (~3.4 kb) was used in a 50 μl reaction according to protocols provided by the supplier. One tenth of the reaction mixture (5 μl) was used in each subsequent binding reaction. Binding assay was carried out by combining the elongin C-containing mixture and 100 ng of the resin-bound d-VHL protein (20 μl of the 50% slurry) in a 50 μl solution containing the binding buffer (see above). The binding mix was incubated at room temperature for 1 h, the supernatant was saved and the resin was rinsed two times 10 min each with 100 μl of the binding buffer. The contents in the supernatant and in the resin after rinsing were subjected to SDS-polyacrylamide gel electrophoresis (a 10–15–20% step gradient gel) and autoradiography. Equivalent amount of Ni-agarose resin was used as negative controls in the binding assay.

Polytene chromosome hybridization

The cloned RT–PCR fragment described above was labeled with digoxigenin using reagents supplied by Roche Molecular Biochemicals. Polytene chromosome *in situ* hybridization was as described (Pardue, 1986).

In situ *detection of gene expression*

RNA *in situ* and immunostaining followed published protocols (Mantrova and Hsu, 1998). Digoxigenin-labeled antisense RNA was synthesized *in vitro* from the *d-VHL* cDNA clone described above using the DIG RNA Labeling Kit from Roche Molecular Biochemicals. The rat anti-Trh polyclonal antibody was a gift from B-Z Shilo of Weizman Institute, Israel, and was used at 1 : 1000 dilution.

RNA interference

PCR primers encompassing the T7 and T3 RNA polymerase promoters were used to amplify the *d-VHL* or the *lacZ* sequences in the pBluescript vector. The resulting fragments were used for *in vitro* RNA synthesis using the Riboprobe Transcription System (Promega). The two single-stranded RNAs were mixed in TE buffer (10 mM Tris-HCl, pH 7/1 mM Na-EDTA) at 0.1 $\mu g/\mu l$ each. The RNA mixture was heat-denatured for 5 min at 80 °C and was allowed to cool down to room temperature over 1 h. In these conditions, the annealing was usually complete as judged by electrophoretic mobility shift. The ds RNA was then ethanol-precipitated and resuspended in injection buffer (5 mM KCl/0.1 mM Na-PO_4, pH 7.8) at a final concentration of 0.2 $\mu g/\mu l$. About 5–10 *pl* was injected into each embryo. Early embryos of the wild-type Oregon-R strain were collected within 2 h of egg-laying. Injection followed the standard procedures (Spradling, 1986). Embryos were immersed in halocarbon oil (Halocarbon Products) to prevent drying and permit free exchange of gases. Injected embryos were allowed to develop at 18 °C for 48 h (low growth temperature helped survival from mechanical trauma) and were directly observed under a light microsocpe.

Over-expression by sense RNA injection

Sense RNA for over-expression experiments were 'capped' to approximate the structure of mRNA *in vivo*. *In vitro* synthesis of capped RNA was essentially the same as described above with the addition of 0.3 mM $m^7G(5')ppp(5')G$ (Stratagene). For the human *VHL* assay, the ORF was cloned into vector pcDNA3 (Invitrogen) between T7 and Sp6 promoters. RNA synthesis was as described above.

Acknowledgments
The authors are grateful to B-Z Shilo for the anti-Trh antibody and GM Technau, DS Watson and J Brieger for comments on the manuscript. B Adryan is supported by a stipend from Studienstiftung des Deutschen Volkes (German National Merit Foundation). This work is supported by grants from Deutsche Forschungsgemeinschaft (German Research Council) and Sonderforschungsbereich (Research Center Grant) 519 (Project C) to HJH Decker; National Cancer Institute (P01CA78582) to TS Papas; and National Institutes of Health (GM57843) to T Hsu.

References

Aso T and Conrad MN. (1997) *Biochem. Biophys. Res. Comm.*, **241**, 334–340.
Beroud C, Joly D, Gallou C, Staroz F, Orfanelli MT and Junien C. (1998) *Nucleic Acids Res.*, **26**, 256–258.
Blankenship C, Naglich JG, Whaley JM, Seizinger B and Kley N. (1999). *Oncogene*, **18**, 1529–1535.
Carmeliet P, Lampugnani MG, Moons L, Breviario F, Compernolle V, Bono F, Balconi G, Spagnuolo R, Oostuyse B, Dewerchin M, Zanetti A, Angellilo A, Mattot V, Nuyens D, Lutgens E, Clotman F, de Ruiter MC, Gittenberger-de Groot A, Poelmann R, Lupu F, Herbert JM, Collen D and Dejana E. (1999). *Cell*, **98**, 147–157.
Crews ST. (1998). *Genes Dev.*, **12**, 607–620.
Fire A, Xu S, Montgomery MK, Kostas SA, Driver SE and Mello CC. (1998). *Nature*, **391**, 806–811.
Folkman J and Shing Y. (1992). *J. Biol. Chem.*, **267**, 10931–10934.
Gnarra JR, Duan DR, Weng Y, Humphrey JS, Chen DY, Lee S, Pause A, Dudley CF, Latif E, Kuzmin I, Schmidt L, Duh FM, Stackhouse T, Chen F, Kishida T, Wei MH, Lerman MI, Zbar B, Klausner RD and Linehan WM. (1996). *Biochim. Biophys. Acta.*, **1242**, 201–210.
Gnarra JR, Tory K, Weng Y, Schmidt L, Wei MH, Li H, Latif F, Liu S, Chen F, Duh FM *et al.* (1994). *Nature Genetics* **7**, 85–90.
Gnarra JR, Ward JM, Porter FD, Wagner JR, Devor DE, Grinberg A, Emmert-Buck MR, Westphal H, Klausner RD and Linehan WM. (1997). *Proc. Natl. Acad. Sci.*, **94**, 9102–9107.
Henikoff S and Henikoff JG. (1992). *Proc. Natl. Acad. Sci.*, **89**, 10915–10919.
Hsu T, Gogos JA, Kirsh SA and Kafatos FC. (1992). *Science*, **257**, 1946–1950.
Iliopoulos O, Ohh M and Kaelin Jr WG. (1998). *Proc. Natl. Acad. Sci.*, **95**, 11661–11666.
Isaac DD and Andrew DJ. (1996). *Gene Dev.*, **10**, 103–117.
Iwai K, Yamanaka K, Kamura T, Minato N, Conaway RC, Conaway JW, Klausner RD and Pause A. (1999). *Proc. Natl. Acad. Sci.*, **96**, 12436–12441.
Jarecki J, Johnson E and Krasnow MA. (1999). *Cell*, **99**, 211–220.
Kaelin Jr WG and Maher ER. (1998). *Trends Genet.*, **14**, 423–426.
Kamura T, Koepp DM, Conrad MN, Skowyra D, Moreland RJ, Iliopoulos O, Lane WS, Kaelin Jr WG, Elledge SJ, Conaway RC, Harper JW and Conaway JW. (1999). *Science*, **284**, 657–661.
Kennerdell JR and Carthew RW. (1998). *Cell*, **95**, 1017–1026.
Kibel A, Iliopoulos O, DeCaprio JA and Kaelin Jr WG. (1995). *Science*, **269**, 1444–1446.
Koochekpour S, Jeffers M, Wang PH, Gong C, Taylor GA, Roessler LM, Stearman R, Vasselli JR, Stetler-Stevenson WG, Kaelin Jr WG, Lineham WM, Klausner RD, Gnarra JR and Vande Woude GF. (1999). *Mol. Cell. Biol.*, **19**, 5902–5912.
Latif F, Tory K, Gnarra J, Yao M, Duh FM, Orcutt ML, Stackhouse T, Kuzmin I, Modi W and Geil L. (1993). *Science*, **260**, 1317–1320.
Leung DW, Cachianes G, Kuang WJ, Goeddel DV and Ferrara N. (1989). *Science*, **246**, 1306–1309.
Lisztwan J, Imbert G, Wirbelauer C, Gstaiger M and Krek W. (1999). *Genes Dev.*, **13**, 1822–1833.
Liu Y and Montell DJ. (1999). *Development*, **126**, 1869–1878.
Mantrova EY and Hsu T. (1998). *Genes Dev.*, **12**, 1166–1175.
Maxwell PH, Dachs GU, Gleadle JM, Nicholls LG, Harris AL, Stratford IJ, Hankinson O, Pugh CW and Ratcliffe PJ. (1997). *Proc. Natl. Acad. Sci. USA*, **94**, 8104–8109.
Maxwell PH, Wiesener MS, Chang GW, Clifford SC, Vaux EC, Cockman ME, Wykoff CC, Pugh CW, Maher ER and Ratcliffe PJ. (1999). *Nature*, **399**, 271–275.
Okuda H, Hirai S, Takaki Y, Kamada M, Baba M, Sakai N, Kishida T, Kaneko S, Yao M, Ohno S and Shuin T. (1999). *Biochem. Biophys. Res. Comm.*, **263**, 491–497.
Pardanaud L and Dieterlen-Lievre F. (1993). *Cell Adhesion Comm.*, **1**, 151–160.
Pardue ML. (1986). *Drosophila, A Practical Approach.* Roberts DB (ed.). IRL Press: Oxford, England, pp. 111–137.
Pause A, Peterson B, Schaffar G, Stearman R and Klausner RD. (1999). *Proc. Natl. Acad. Sci. USA*, **96**, 9533–9538.
Risau W. (1997). *Nature*, **386**, 671–674.

Samakovlis C, Hacohen N, Manning G, Sutherland DC, Guillemin K and Krasnow MA. (1996). *Development*, **122**, 1395–1407.
Schoenfeld A, Davidowitz EJ and Burk RD. (1998). *Proc. Natl. Acad. Sci. USA*, **95**, 8817–8822.
Shweiki D, Itin A, Soffer D and Keshet E. (1992). *Nature*, **359**, 843–845.
Spradling AC. (1986). *Drosophila, A Practical Approach*. Roberts DB. (ed.). IRL Press: Oxford, England, pp. 175–197.
Stebbins CE, Kaelin Jr WG and Pavletich NP. (1999). *Science*, **284**, 455–461.
Stroumbakis ND, Li Z and Tolias PP. (1994). *Gene*, **143**, 171–177.
Sutherland D, Samakovlis C and Krasnow MA. (1996). *Cell*, **87**, 1091–1101.
Tanaka-Matakatsu M, Uemura T, Oda H, Takeichi M and Hayashi S. (1996). *Development*, **122**, 3697–3705.
Wang GL, Jiang BH, Rue EA and Semenza GL. (1995). *Proc. Natl. Acad. Sci. USA*, **92**, 5510–5514.
Wilk R, Weizman I and Shilo BZ. (1996). *Gene Dev.*, **10**, 93–102.
Wingrove JA and O'Farrell PH. (1999). *Cell*, **98**, 105–114.